



Fabrication of H₂S Gas Sensor Based on Ppy/CuO and Ppy/SnO₂ Nanocomposites at Room Temperature



A. M. Al-Sabagh¹, Khalid I. Kabel^{1*}, T. Zaki¹, A. M. Badawi¹, Adel A.-H. Abdel-Rahman², Walaa S. Gado¹

¹Egyptian Petroleum Research Institute (EPRI), P.O. 11727, Nasr City, Cairo, Egypt.

²Department of Chemistry, Faculty of Science, Menoufia University, Egypt.

THE existence of Hydrogen sulfide (H₂S) during the petroleum production and its high risks is the main reason to develop a smart, cheap and flexible device for H₂S monitoring. This article is focusing on developing electrochemical sensors, which seems to have a promising potential. Polypyrrole (Ppy) and its two composites were prepared; Ppy doped with Copper oxide (CuO) nanoparticles (Ppy/CuO) and Ppy doped with Tin oxide (SnO₂) nanoparticles (Ppy/SnO₂) via in-situ polymerization approach. The characterizations of these nanocomposites were confirmed by Fourier Transform Infrared spectroscopy (FTIR), X-ray diffraction (XRD), Dynamic Light Scattering (DLS) and High-Resolution Transition Electron Microscopy (HR-TEM). The testing of these nanocomposites towards the monitoring of H₂S gas at different concentrations was carried out in the term of electrical resistance changes. From the data; it was found that the response at 1000 ppm H₂S gas concentration was ranked as; Ppy 0.12 %. Ppy/CuO 4.7 %. Ppy/SnO₂ 53.2 %.

Keywords: H₂S gas, Gas sensors, Polypyrrole, Nanocomposites, Metal oxide nanoparticles.

Introduction

H₂S is an explosive, flammable, and toxic gas. Various respiratory symptoms could be resulted from the exposure to low concentrations of H₂S. On the other hand serious health effects and death results from its high exposure level [1]. The fast and precise detection of such toxic gas at low concentrations is a demand to protect lives, save environment and equipments [2].

H₂S occurs mostly from the petroleum crude, natural gas, volcanoes, sewage, hot springs, and coke ovens [3]. Besides the odor nuisance often resulting from H₂S emissions, acid rains also consider a dangerous form of H₂S emissions which creates when clean rains react with the air pollutants, such as (SO_x), (NO_x), and (CO₂). Then, acid rain falls to the Earth and damages all of the plants, water, soil, animals, and construction

materials [4]. Furthermore, H₂S is dangerous not only for human but also for equipments at certain concentrations. Furthermore, existence of H₂S gas in presence of aqueous media lead to acid formation causing serious damage in pipelines with increasing the corrosion rate of stress crack corrosion (SCC) [5].

The recorded limits for H₂S analysis in air are 10 mg/m³ (6.7 ppm) for GC or 0.2 mg/m³ (130 ppb) in spectrophotometry. However, these methods are expensive, difficult, and unsuitable for large scale performing [6]. Recently, the most commercially sensors for H₂S detection employ both electrochemical and semiconductor, which have a detection limit of about 1 ppm. Although, these are affected by humidity, high power consumption, and needed continuous recalibrations, especially when used in portable equipments [7]. The inexpensive method for

*Corresponding author e-mail: drkhalid1977@yahoo.com; Tel.: +20 2 22745902; fax: +20 2 22747433.

Received 16/12/2019; Accepted 6/1/2020

DOI: 10.21608/ejchem.2020.21041.2257

© 2020 National Information and Documentation Center (NIDOC)

sensing H_2S in air at different concentrations up to thousands of ppm is the 3-electrode configuration with liquid electrolyte as an electrochemical sensor type. Indeed, the cost of the electrochemical sensor is about 30 US dollars[8]. The factors which can be affected on the sensor selectivity are the sensing material, target gas in addition to the design and material type of both the substrate and electrode [9].

Nowadays, there is a dramatically rising of the number of gases that can be monitored by gas sensors such as H_2S , NH_3 and air pollutants like NO_x , SO_x and CO_2 which are the main cause of the serious environmental disasters over the last years [10]. The chemical gas sensors of different sensing materials have been applied as a thin or thick film. Many studies have been reported for the semiconducting metal oxides like CuO , WO_3 , CeO_2 , ZnO and SnO_2 as a Thin films for gas monitoring [11-12]. Many problems of the metal oxide-based sensors like the low selectivity, high operating temperature, short life time, high-power consumption which limit their applications[13]. So, the conducting polymers, such (Polypyrrole (Ppy), polyaniline (PANI), polythiophene (PTh)) are used as sensing materials because of their sensitivity and reactivity to change their electrical characteristics when exposed to some gases. The common advantage of conducting polymers is their low cost, flexibility, facile application and ease-fabrication. As a result, focused research has been directed to the gas sensors related to conducting polymers. For enhancing the sensing performance, conducting polymers hybrid nanomaterials are used to overcome the basic limitations of film-based sensors [14]. Hybrid polymer nanocomposites have attractive development strategies to improve the individual components limitations and improvement the reactivity of mechanical actuators. The most improvements in sensor performance depend on the high surface area properties of nanomaterials. Moreover, the sensing mechanism of gas sensors is basically based on the changes in the electrical resistivity of the sensing materials for the target gases with its surface [15].

This work is focusing on two targets, the first one is to prepare chemical sensor based on Ppy nanocomposites and confirm their structure. The second target is to evaluate these composites as chemical sensors for H_2S . The Keithley electrometer should be used to record the response of the fabricated sensors in the term of electrical

resistance. Our attention might be extended to discuss the results on the basis of electrochemistry and electron transfer.

Experimental

Raw Materials

Stannous chloride dihydrate ($SnCl_2 \cdot 2H_2O$), Copper (II) Chloride dihydrate ($CuCl_2 \cdot 2H_2O$), ammonia solution (NH_4OH), silver nitrate ($AgNO_3$), Pyrrole (C_4H_5N) monomer (density; $0.97g/cm^3$ at $20^\circ C$, a melting point $24^\circ C$ stored in dark at $0^\circ C$). Analytical grade (Iron (III) chloride hexahydrate- $FeCl_3 \cdot 6H_2O$). All chemicals were supplied from sigma Aldrich. All solutions were prepared in distilled water. Different concentrations of H_2S gas canisters were purchased as calibration standard gas cylinders from AG Gases Ltd, UK.

Preparation of Polypyrrole

In two necked flask a solution of 27 gm. (0.1 M) of oxidizing agent $FeCl_3 \cdot 6H_2O$ was added slowly to 100 ml (0.15 M) of Pyrrole monomer dissolved in 50 ml distilled water under continuous stirring with nitrogen atmosphere in ice bath to kept temperature at $0^\circ C$ for 5 hrs. The reaction mixture was kept un-agitated for 24 hr. until the black powder of Ppy was settled down. The obtained precipitate powder was filtered out under vacuum and washed many times to remove any impurities. The Polypyrrole precipitate was dried at $100^\circ C$ for 4 hr. [16], the schematic illustration of the in situ-polymerization procedure was shown in Fig.1.

Preparation of the CuO and SnO_2 Nanoparticles

19 gm. (0.1 M) of $SnCl_2 \cdot 2H_2O$ was dissolved in 100 ml distilled water. After complete dissolution, about 50 ml of (0.5 M) NH_4OH solution was added to adjust the pH value at 8. A white gel precipitate was immediately appeared. It was allowed to settle at room temperature for 24 hr. Then, filtered and washed by distilled water several times till a clear solution was obtained, and no chloride ions were detected using $AgNO_3$ solution. The obtained precipitate was dried for 24 hr. at $70^\circ C$. The dried powder was milled and calcinated at $600^\circ C$ for 4 hr.

The CuO NPs was prepared by Applying the same procedure as SnO_2 preparation; 50 ml of (0.5 M) NH_4OH solution was added slowly to the aqueous solution of 100 ml of (0.1 M) $CuCl_2 \cdot 2H_2O$ at room temperature with continuous stirring until the greenish blue precipitate was formed at pH value about 8. The precipitate was washed several

times until no chloride ions were detected. Then the precipitate was filtered and dried for 6 hr. at 100 °C and calcinated at 500 °C for 3 hr.

Preparation of the Ppy/CuO and Ppy/SnO₂ Nanocomposites

Following the same procedure of Polypyrrole preparation, A solution of 100 ml (0.1M) of Pyrrole monomer was mixed with CuO or SnO₂ nanoparticles at (10, 20, or 30) % per weight individually with continuous stirring for 30 min. 27 gm. (0.1 M) of oxidizing agent FeCl₃·6H₂O was added dropwise with continuous stirring in ice bath (0 °C) under nitrogen flow for 4 hr. The black precipitates of Ppy/CuO and Ppy/SnO₂ nanocomposites were filtered and dried at 60°C for 6hr. and at 50 °C for 3 hr. respectively.

Setup of the Gas Sensing Unit

In order to detect the gas response, a computer assisted designed interdigitated electrode separated by 1mm. from its all sides, was fabricated on a printed circuit board (PCB). In order to form the deposition paste; the solution of sensing material powder was mixed with polyethylene glycol as a binder and spread over using drop casting technique uniformly then allowed to dry under vacuum at room temperature for 20h. A Lab-made conical sealed glass chamber of 500 ml with gas inlet port was installed; the fabricated sensor was fitted inside the chamber firmly with the proper electrical connections. The H₂S gas of different concentrations (100, 400, 600, and 1000 ppm), was passed through the chamber at room temperature.

The electrical resistance changes were recorded as a result of the reaction of the sensing materials with H₂S gas, at a constant voltage 0.1 V DC provided from electrical power supply, for every 5 seconds by the computer assisted 6-digit Keithley 6514 System Electrometer. The Keithley electrometer was connected to the computer via GBIP interface. The H₂S gas concentrations which were used in our lab tests were obtained in 1-liter tedlar bag capacity then it was connected to the chamber.

The gas response was calculated by the following equation [17];

$$\text{Response \%} = \frac{R_a - R_g}{R_a} \times 100 \dots \dots \dots (1)$$

where, R_a is the initial resistance in the presence of air, R_g is the resistance in the presence of the H₂S gas.

To study the gas effect on the sensor response, the resistance was measured in the air and in the flow of H₂S gas at ambient temperature. The sensor was placed in the chamber. The H₂S gas flow started to fill the chamber until complete occupation, during the test time the electrometer recorded the resistance changes every 5 sec. for 15 min. then the chamber was allowed to air exposure before the second cycle of H₂S exposure. The experimental setup was illustrated in Fig.2.

Characterization Techniques

The crystallography of the synthesized

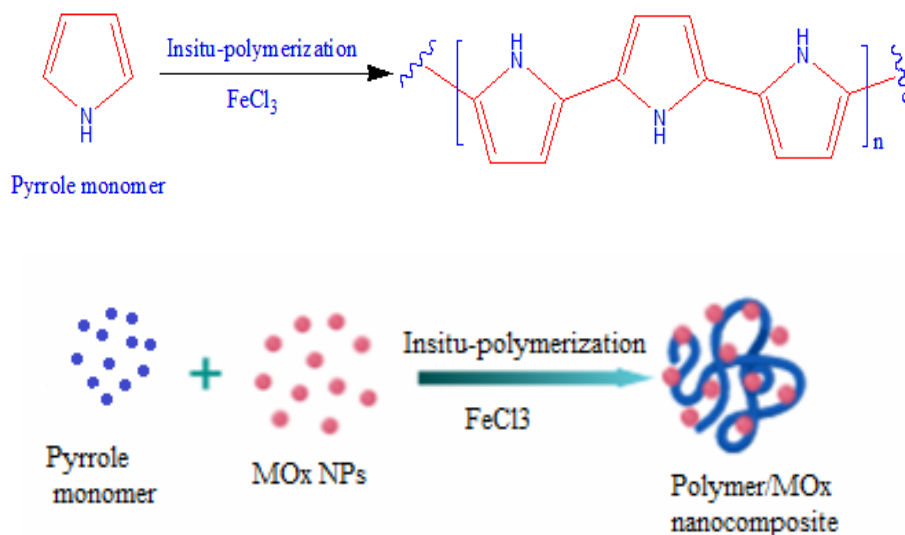


Fig. 1. Scheme of polymerization reaction.

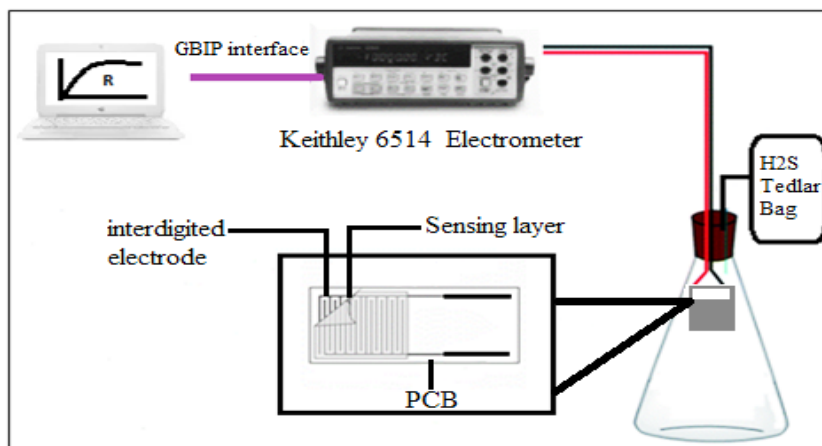


Fig. 2. The experimental setup for gas monitoring with Interdigitated electrode design.

nanoparticles were confirmed by X-ray Diffraction (XRD) using model (X'Pert Pro) 2 range from 5°-90° conditions 40 mA, 40 kV, and wave length of Copper $K\alpha_1$ at 1.54 Å, with a Cu-K α radiation ($\lambda = 1.5406$ Å) Diffractometer. The particle size and the morphology of the prepared nanoparticles were characterized using the High Resolution Transmission Electron Microscopy (HR-TEM, JEOL JEM-2100F, Japan, 200 KV). The particle size distribution was obtained using the Dynamic Light Scattering (DLS) with a laser angle 90° at 25°C, (Zetasizer Nano-ZS90 instrument, Malvern Co., UK). The chemical structure and function groups of the prepared Polypyrrole were characterized by a Nicolet iS10 FT-IR spectrophotometer (Thermo Fisher Scientific, USA) in a wavenumber range 500-4000 cm^{-1} . The Polypyrrole molecular weight was recorded using Gel Permeation Chromatography (GPC), a GPC-water 2410 with reflective index detector using 4 columns styragel HR THF 7.8 \times 300 mm, calibrated by PS standard, supported a water 515 HPLC pump. The electrical measurements and the responses of the gas sensors were monitored using (Keithley instrument, Inc. USA) a Keithley source measurement unit (6514). The electrometer was interfaced to the computer via GPIB interface.

Results and Discussion

Structure Characterization and Morphology study of Ppy, CuO NPs and SnO₂ NPs, Ppy/CuO and Ppy/SnO₂ Nanocomposites.

The prepared Polypyrrole function groups were identified using FT-IR as shown in Fig.3. The spectrum revealed that; the N-H stretching peak at 3470 cm^{-1} . Whereas the peaks at 2989 cm^{-1} related to -C-H, 1392 cm^{-1} and 1565 cm^{-1} are related to

C-N and C=C respectively. A peak at 1178 cm^{-1} was related to =C-C. All these peaks are the main characteristic of Ppy.

Also, the prepared Polypyrrole was determined by GPC. The solution of the prepared Polypyrrole was dissolved in THF GPC grade "flow rate 1ml/min", the analysis recorded that the molecular weight $M_w = 10000$ and the polydispersity was 3.6.

The XRD pattern of the prepared Ppy is seen in Fig.4a. It can be observed that there wasn't any sharp peak detected in the range of 1-40° which confirmed to the amorphous structure of the Ppy. A broad pattern about 25° is corresponding to Ppy and it is a typical for the doped structure of Ppy.

On the other hand, the XRD pattern of the CuO NPs was in monoclinic phase which shown in the Fig.4b. The average crystallite size was calculated by Debye Scherer's equation;

$$D = \frac{0.9 \lambda}{\beta \cos \theta} \dots \dots \dots (2)$$

where D is the crystal size, λ is the X-ray wavelength, β is the full width at half maximum of the diffraction peak, and θ is the Bragg diffraction angle of the diffraction peaks; and found to be 55 nm. According to (JCPDS card no. 80-0076), the exhibited diffraction peaks at $2\theta = 32.52^\circ$ (1 1 0), 35.51° (-1 1 1), 38.74° (111), 46.27° (-1 1 2), 48.77° (-2 0 2), 53.59° (0 2 0), 58.32° (2 0 2), 61.57° (-1 1 3), 66.25° (-311) and 68.07° (2 2 0) related to the different planes of monoclinic phase of CuO NPs.

Furthermore, The XRD of the SnO₂ NPs

is shown in **Fig.4** according to (JCPDS card no.41-1445), the peaks showed at 2θ values of 26.5° (1 1 0), 33.7° (1 0 1), 37.8° (2 0 0), 51.9° (2 1 1), 54.8° (2 2 0), 61.8° (3 1 0) and 65.8° (3

0 1) confirmed that the product is of SnO₂ and in good agreement with the literature. The average particle size D was found to be 17 nm.

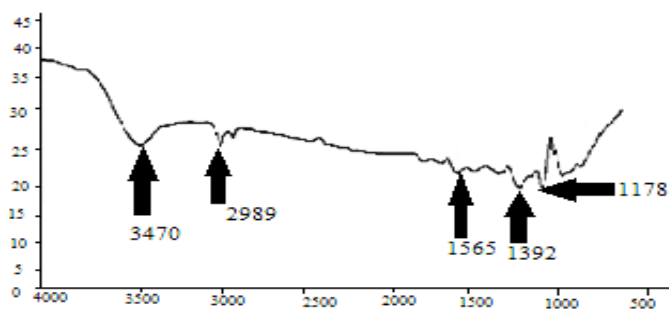


Fig. 3. FTIR spectra of Polypyrrole.

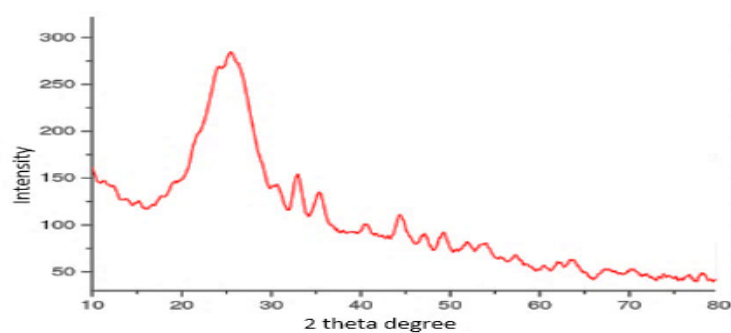


Fig. 4a. XRD patterns of Ppy.

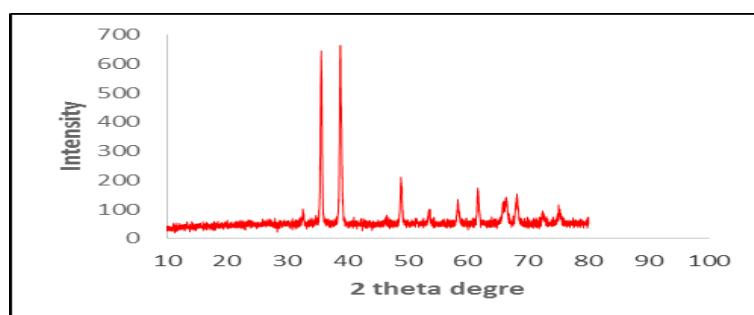


Fig. 4b. XRD patterns of CuO NPs.

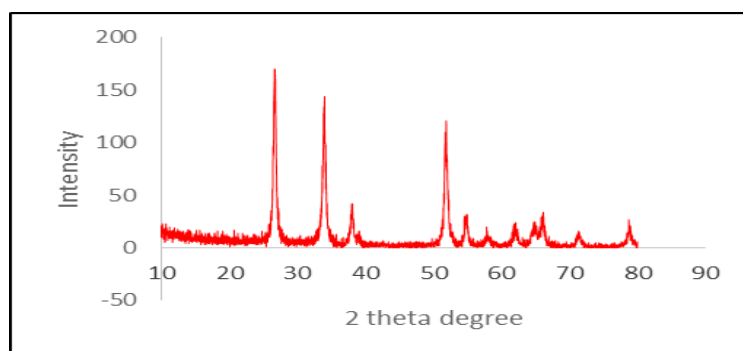


Fig. 4c. XRD patterns of SnO₂ NPs.

The particle size distribution of the prepared NPs was measured using DLS. It was observed from the data that the particle size of the prepared CuO NPs was in range of 50 to 110 nm. As illustrated in **Fig.5a**. It also seen that the presence of the higher number of particles within 90 nm. The polydispersity index value (PDI) of the suspended particles was found 0.154, which

is below the acceptable range of 0.7. PDI values are ranging from 0 to 1; the value lower than 0.05 indicates a monodispersed phase, whereas the value higher than 0.7 indicates a broad particle size distribution. The particle size distribution of the prepared SnO₂ NPs was in the range of 15 to 77 nm. as shown in **Fig.5b**, the higher number of particles was located within 71 nm. The PDI of the suspension was found to be 0.296.

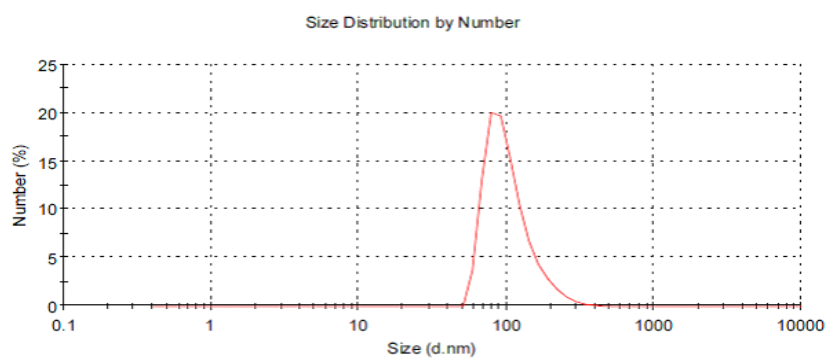


Fig. 5a. Particle size distribution of CuO NPs.

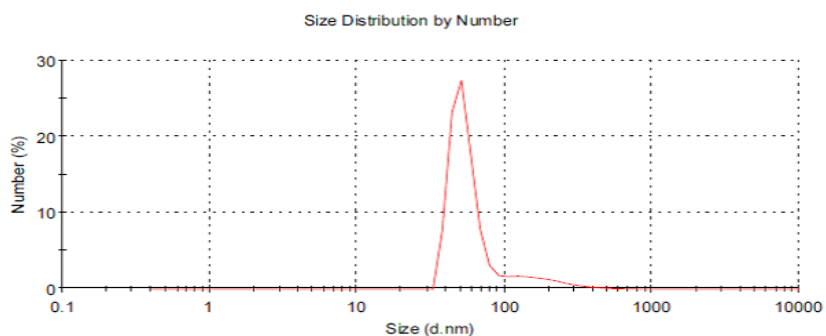


Fig. 5b. Particle size distribution of SnO₂ NPs.

The shape, size and morphology of the fabricated MO_x NPs were detected using HRTEM as shown in **Fig. 6a, b**. The samples were prepared by putting a tiny droplet of sonicated water-based MO_x NPs suspension on a carbon supported copper grid. The CuO NPs have a tetragonal shape with an average size of 50 to 60 nm. It seems as clustered attributed to the particles aggregation affected by the low evaporation rate of the solvent. At high magnification all observed CuO NPs exhibit atomic fingers with specific orientations. These observations mean that the synthesized CuO NPs have high crystallinity with random orientation. Moreover, the HRTEM images of the prepared SnO₂ NPs shows a spherical structure with a tiny size ranged of 6-11 nm.

The HRTEM images of the Ppy show that the particles of Ppy are attached to each other as clusters. Furthermore, the SAED pattern shows the uniform central and diffraction spots of the Ppy indicating its amorphous structure as shown in **Fig. 6c**.

Finally, the HRTEM images of Ppy/CuO and Ppy/SnO₂ nanocomposites as seen in **Fig. 6d, f** respectively, indicate that the morphology of the hybrid nanocomposites is microstructure with uniform distribution of NPs in Ppy matrix which confirm that the in-situ polymerization produced non-aggregated matrix. The uniform distribution of NPs in the Ppy matrix improves the conductivity properties. The shape of NPs didn't change in the nanocomposites. Thus, the nanocomposites microstructure improved the surface roughness leading to increase the surface reactive pores [20].

Gas Sensing Properties of Ppy and Ppy/MO_x Nanocomposites.

The response of the fabricated sensors was calculated according to eq.(1): The exposure of sensors to H₂S gas which is an electron-donor leading to decrease the resistivity so the response R (%) has always positive sign. Thus, the decrease in the resistance of Ppy/CuO and Ppy/SnO₂ nanocomposites after the exposure to H₂S gas is consistent with the decrease in the resistance of the Ppy that caused by reducing in the electron hopping. It was observed that the change in the dynamic response for all fabricated sensor started with decrease its resistance, then remained constant for short time and the recovery time

was obtained by opening the gas test unit to the ambient atmosphere [18,19].

After inspecting the drawn data in **Fig. 7** it was observed that the best sensing material response to 100 ppm H₂S gas exhibit by the Ppy/SnO₂(30) followed by Ppy/CuO(30) then Ppy/SnO₂ (10, 20), Ppy/CuO (10, 20) and Ppy sensors. Therefore, the samples Ppy/SnO₂ (30) and Ppy/CuO (30) were selected to apply sensing tests for H₂S gas at different concentrations (100, 400, 600 and 1000 ppm) at room temperature.

Figure 8 shows the response of Ppy, Ppy-CuO (30), and Ppy/SnO₂ (30) at H₂S gas concentrations of 100 ppm, 400 ppm, 600 ppm and 1000 ppm. The Ppy/SnO₂ (30) nanocomposite achieved the maximum sensor response towards 1000 ppm H₂S 53.2 %. At the same time the Ppy/CuO (30) sensor recorded 4.7 % and the Ppy sensor pronounced 0.12 %.

The dynamic response of Ppy/SnO₂(30) nanocomposite sensor towards H₂S and the recovery time was illustrated in **Fig. 9**.

Mechanism of Sensing

The high surface morphology of nanomaterials and the density of the porous structure are the main factors affecting on the sensor response within the sensing layer diffusion towards the H₂S gas. Also, these characteristics increase the reaction rate between H₂S and the positive charges along the Ppy. [20-21]. Both of Ppy/CuO and Ppy/SnO₂ nanocomposites are a resistor-type sensor where the sensing mechanism of this sensor depends on the changes in their electrical resistivity. For Ppy sensor, when it is exposed to electron donating gases like H₂S, a redox reaction occurs and its effective number of charge carrier reduced, thus decreased its resistance [22-24]. The large number of grains is leading to large effective surface area available for adsorption of gas molecules and high porosity. The gas sensing mechanism is explained according to the model of potential barrier. The potential barrier is depending on the concentration of the adsorbed oxygen. When the H₂S gas was adsorbed on the surface of the sensing layer the adsorbed oxygen is consumed by reacting with H₂S gas, and the entrapped electrons are returned to the SnO₂ grains resulting in a decrease of the potential barrier and the resistance. [25,26].

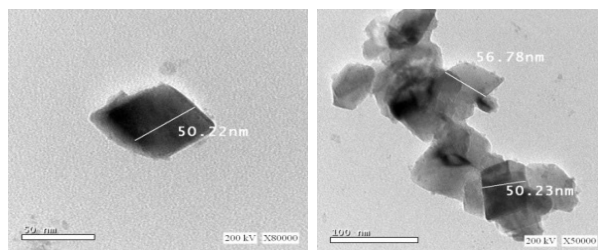


Fig. 6a. HRTEM images of CuO NPs.

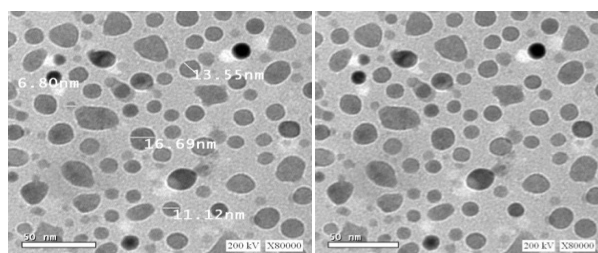


Fig. 6b. HRTEM images of SnO₂ NPs.

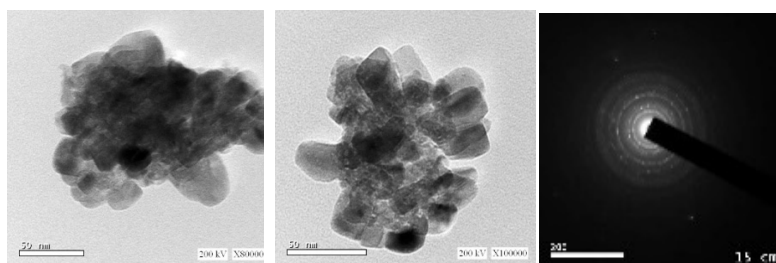


Fig. 6c. HRTEM images and SAED of Polypyrrole.

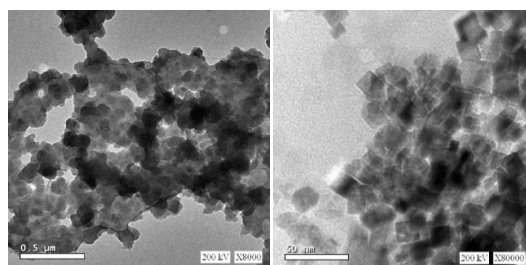


Fig. 6d. HRTEM images of Ppy/CuO nanocomposite.

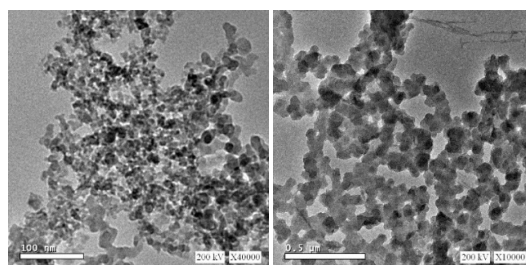


Fig. 6f. HRTEM images of Ppy/SnO₂ nanocomposite.

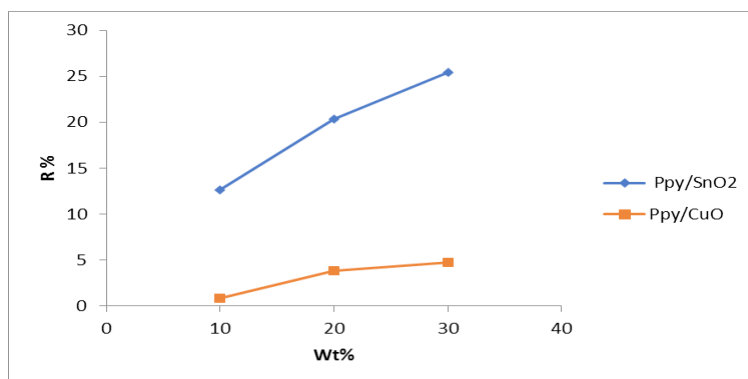


Fig. 7. The 100 ppm H₂S gas response of different doping ratios of NPs to Polypyrrole.

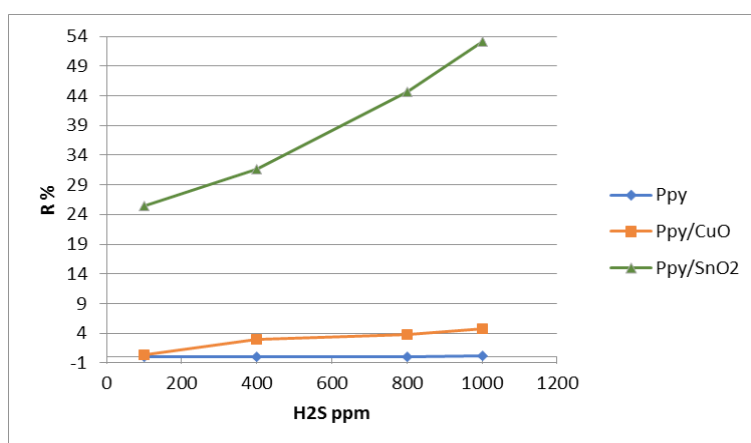


Fig. 8. The sensing response of Ppy, Ppy/CuO and Ppy/SnO₂ sensor towards different concentrations of H₂S gas.

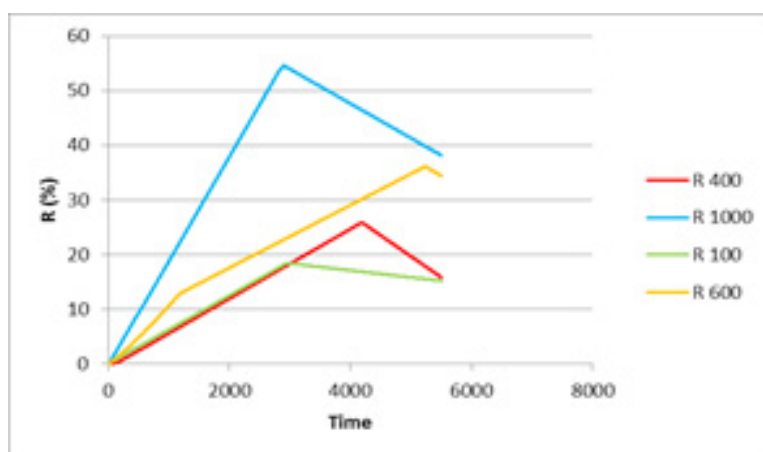
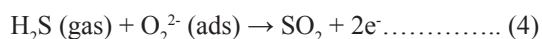
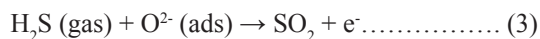


Fig. 9. The dynamic sensing response of Ppy/SnO₂ sensor towards different concentrations of H₂S gas with time.

It's known that the reducing gases as H₂S have a proton doping effect towards several polymers such as Ppy as a p-type semiconductor [27-31]. The absorbed H₂S gas has been dissociated into H⁺ and (HS⁻ or S²⁻) on the surface of the nanocomposites. The Ppy was protonated by the H⁺ leading to improving its conductivity. On the other hand, the conductivity of the n-type NPs (SnO₂ and CuO) has been enhanced affected by its reaction with the highly reactive dissociated (HS⁻ or S²⁻) which is the strongest logical purposed sensing mechanism [32-36]. Hence, the depletion layer is the region rich of charges, when associated with organic-inorganic (p-n heterostructure) it has two types. The first type existed when the oxygen molecules adsorbed at the surface of NPs, while the second type caused by the p-n heterojunction at the contact interface of Polymer and NPs [37]. These depletion layers were affected by the existed atmosphere. In the air, surface potential barrier was increased referred to the adsorption of the O₂ species at the surface sites and trap electrons from the junction. In case of H₂S gas exposure, the potential barrier in the depletion region decreased due to the back release of electrons to the sensing material surface [36]. The reactions between the H₂S and the adsorbed oxygen molecules can be explained as the following equations :



It's clearly observed that both of the response (R, %) and the response time (T, sec.) of Ppy/SnO₂ nanocomposite was better than among of Ppy/CuO nanocomposite and Ppy. This is referred to the high oxygen vacancies of SnO₂ than CuO which adsorbed more oxygen species leading to decrease the surface potential barrier in addition to the small size of SnO₂ nanoparticles (6-11 nm) compared to CuO (50-60 nm).

Conclusion

The proposed low cost H₂S gas sensor was fabricated based on deposition a sensing layer of the prepared Ppy, Ppy/CuO and Ppy/SnO₂ nanocomposites on the fabricated sensors and its response was detected using Keithley electrometer. The porous structure of the sensing layer pronounced high surface area for the free access of the target gas and also reduce the gas diffusion resistance, leading to satisfied sensitivity. It was shown that the Ppy/SnO₂ sensor exhibited the high response towards 100, 400, 600 and 1000 ppm of H₂S gas (R %, 25.4, 31.6, 44.7 and 53.2 respectively), this is referring to the high selectivity of tin oxide towards the H₂S gas and the high oxygen vacancies of SnO₂ than CuO which adsorbed more oxygen species leading to decrease the surface potential barrier in addition to the small size of SnO₂ nanoparticles (6-11 nm) compared to CuO (50-60 nm).

600 and 1000 ppm of H₂S gas (R %, 25.4, 31.6, 44.7 and 53.2 respectively), this is referring to the high selectivity of tin oxide towards the H₂S gas and the high oxygen vacancies of SnO₂ than CuO which adsorbed more oxygen species leading to decrease the surface potential barrier in addition to the small size of SnO₂ nanoparticles (6-11 nm) compared to CuO (50-60 nm).

References

1. Zhijie L., Ningning W., Zhijie L., Junqiang W., Wei L., Kai S., Yong Q.R. F., and Zhiguo W. Room-temperature high performance H₂S sensor based on porous CuO nanosheets prepared by hydrothermal method. *ACS Appl. Mater. Interfaces*, **8**(32), 20962-20968 (2016).
2. Dongyang X., Rui Z., Xiaoping L., Xiaochuan D., Qihong L., and Taihong W. A highly selective and sensitive H₂S sensor at low temperatures based on Cr-doped α-Fe₂O₃ nanoparticles. *RSC Adv.*, **9**, 4150-4156 (2019).
3. <https://www.osha.gov/SLTC/hydrogensulfide/hazards.html>, November, (2016).
4. <https://www.livescience.com/63065-acid-rain.html>, July, (2018).
5. Davoodi A., Pakshir M., Babaiee M., Ebrahimi G. R. A comparative H₂S corrosion study of 304L and 316L stainless steels in acidic media. *Corrosion Science*, **53**, 399-408 (2011).
6. World Health Organization (WHO). Concise International Chemical Assessment Document 53, Hydrogen sulfide: Human health aspects. WHO: Geneva, Switzerland (2003), <http://www.who.int/ipcs/publications/cicad/en/cicad53.pdf>.
7. Pandey S. K., Kim K.H., Tang K.T. A review of sensor-based methods for monitoring hydrogen sulfide. *Trends Anal. Chem.*, **32**, 87-99 (2012).
8. Membrapor, AG, Switzerland: Electrochemical gas sensors for detecting H₂S. Available online: <http://www.membrapor.ch/> (accessed on 23 January 2017).
9. Alphasense Ltd., United Kingdom. Alphasense, Ltd, United Kingdom.: Alphasense hydrogen sulphide gas sensors. Available online: <http://www.alphasense.com/index.php/products/hydrogen-sulfide-safety/> (accessed on 23 January 2017).
10. MdA.H. K., Mulpuri V. R., and Qiliang L. Recent Advances in Electrochemical Sensors for Detecting Toxic Gases: NO₂, SO₂ and H₂S. *Sensors*, **19**(4), 905 (2019).

11. Li Z., Niu X., Lin Z., Wang N., Shen H., Liu W., Sun K., Fu Y.Q., Wang Z. Hydrothermally synthesized CeO₂ nanowires for H₂S sensing at room temperature. *J. Alloy. Compd.*, **682**, 647–653 (2016).
12. Drobek M., Kim J.H., Bechelany M., Vallicari C., Julbe A., Kim S.S. MOF-Based Membrane Encapsulated ZnO Nanowires for Enhanced Gas Sensor Selectivity. *ACS Appl. Mater. Interfaces*, **8**, 8323–8328 (2016).
13. Kneer J., Knobelspies S., Bierer B., Wöllenstein J., Palzer S. New method to selectively determine hydrogen sulfide concentrations using CuO layers. *Sens. Actuators B Chem.*, **222**, 625–631 (2016).
14. Bandgar D. K., Navale S. T., Nalage S. R., Mane R. S., Stadler F. J., Aswal D. K., Gupta S. K., Patil V. B. Simple and low-temperature polyaniline-based flexible ammonia sensor: a step towards laboratory synthesis to economical device design. *J. Mater. Chem. C*, **3**, 9461 (2015).
15. Suhail M.H., Abdullah O. Gh., Ghada A. K. Hydrogen sulfide sensors based on PANI/f-SWCNT polymer nanocomposite thin films prepared by electrochemical polymerization. *Journal of Science: Advanced Materials and Devices*, **4**, 143–149 (2019).
16. Murugendrappa M. V., Ambika Prasad M.V.N. Chemical synthesis, characterization, and direct-current conductivity studies of polypyrrole/ γ -FeO composites. *J. App. Poly. Sci.*, **103**, 2797–2801 (2007).
17. Cullity B.D. Elements of X-ray Diffraction, 3rd ed. Addison Wesley Publishing Company Inc.: London, UK (1978).
18. Simon C. E., Florea O. G., Stanoiu A. Gas sensing mechanism involved in H₂S detection with NiO loaded SnO₂ gas sensors. *Romanian Journal of Information Science and Technology*, **20** (4) 415–425 (2017).
19. Mubeen S., Zhang T., Chartuprayoon N., Rheem Y., Mulchandani A., Myung N. V., Deshusses A. M. Sensitive Detection of H₂S Using Gold Nanoparticles Decorated SWNTs. *Anal. Chem.*, **82** (1), 250–257 (2010).
20. Khorami H. A., Eghbali A., Keyanpour-Rad M., Vaezi M. R., Kazemzad M. Ammonia sensing properties of (SnO₂-ZnO)/polypyrrole coaxial nanocables. *J. Mater. Sci.*, **49**, 685–690 (2014).
21. Mirzaei A., Kim S. S., Kim H.W. Resistance-based H₂S gas sensors using metal oxide nanostructures: A review of recent advances. *Journal of Hazardous Materials*, **5**, (357) 314–331 (2018).
22. Hernandez S. C., Chaudhuri D., Chen W., Myung N.V. Single Polypyrrole Nanowire Ammonia Gas Sensor. *Electroanalysis*, **19**, 2125–2130 (2007).
23. Yoon H., Chang M., Jang J. Sensing Behaviors of Polypyrrole Nanotubes Prepared in Reverse Microemulsions: Effects of Transducer Size and Transduction Mechanism. *J. Phys. Chem. B*, **110**, 14074 (2006).
24. Gangopadhyay R., De, A. Conducting polymer composites: novel materials for gas sensing. *Sens. Actuators B*, **77**, 326 (2001).
25. Liu J., Huang X., Ye G., Liu W., Jiao Z., Chao W., Zhou Z., Yu Z., H₂S Detection Sensing Characteristic of CuO/SnO₂ Sensor. *Sensors*, **3**, 110 (2003).
26. Waghuley S. A. Gas Sensitive Electrical Conduction of Polypyrrole Modified SnO₂-Al₂O₃ Sensors. Ph.D. Thesis, (Sant Gadge Baba Amravati Univ., Amravati., India 2008).
27. Agbor N. E., Petty M. C., Monkman A. P. An optical gas sensor based on polyaniline Langmuir-Blodgett films. *Sens. Actuators, B*, **41**, (1) 137–141. (1997).
28. Lakard B., Carquigny S., Segut O., Patois T., Lakard S. Gas Sensors Based on Electrodeposited Polymers. *Metals*, **5**, 1371–1386 (2015).
29. Garg R., Kumar V., Kumar D., Chakarvarti S. Polypyrrole Microwires as Toxic Gas Sensors for Ammonia and Hydrogen Sulphide. *J. Sens. Instrum.*, **3**, 1–13 (2015).
30. Geng L., Wang S., Zhao Y., Li P., Zhang S., Huang W., Wu S. Study of the primary sensitivity of polypyrrole/r-Fe₂O₃ to toxic gases. *Mater. Chem. Phys.*, **99**, 15–19 (2006).
31. Krivan E., Visy C., Dobay R., Harsanyi G., Berkesi O. Irregular response of the polypyrrole films to H₂S. *Electroanalysis*, **12**, 1195–1200 (2000).
32. Xue X., Xing L., Chen Y., Shi S., Wang Y., Wang T. Synthesis and H₂S Sensing Properties of CuO-SnO₂ Core/Shell PN-Junction Nanorods. *J. Phys. Chem. C*, **112**, 12157–12160 (2008).
33. Shirsat M., Bangar M., Deshusses M., Myung N., Mulchandani A. Polyaniline nanowires-gold nanoparticles hybrid network based chemiresistive hydrogen sulfide sensor. *Appl. Phys. Lett.*, **94**, 083502–083504 (2009).

34. Zhang S., Zhang P., Wang Y., Ma Y., Zhong J., Sun X. Facile Fabrication of a Well-Ordered Porous Cu-Doped SnO₂ Thin Film for H₂S Sensing. *ACS Appl. Mater. Interfaces*, **6**, 14975-14980 (2014).
35. Wang Y., Liu B., Xiao S., Wang X., Sun L., Li H., Xie W., Li Q., Zhang Q., Wang T. Low-Temperature H₂S Detection with Hierarchical Cr-Doped WO₃ Microspheres. *ACS Appl. Mater. Interfaces*, **8**, 9674-9683 (2016).
36. Marichy C., Donato N., Willinger M., Latino M., Karpinsky D., Yu S., Neri G., Pinna N. Tin Dioxide–Carbon Heterostructures Applied to Gas Sensing: Structure-Dependent Properties and General Sensing Mechanism. *J. Phys. Chem. C*, **117** (38), 19729-19739 (2013).
37. Russo P. A., Donato N., Leonardi S. G., Baek S., Conte D. E., Neri G., Pinna N. Room-temperature hydrogen sensing with heteronanostructures based on reduced graphene oxide and tin oxide. *A. Chem. Int. Ed.*, **51**, 11053-11057 (2012).

تصنيع مستشعر لغاز كبريتيد الهيدروجين (H₂S) معتمد على Ppy/CuO , Ppy/ SnO₂ نانوكومبوزيت في درجة حراره الغرفه

احمد محمد الصباغ^١ ، خالد اسماعيل قابل^{١*} ، تامر زكي شراره^١ ، عبد الفتاح محسن بدوي^١ ، عادل عبد الهادي نصار^٢ و ولاء شعبان جادوا^١
^١معهد بحوث البترول - مدينة نصر - القاهرة - مصر .
^٢كلية العلوم - جامعة المنوفية - المنوفية - مصر .

نتيجه لتواجد غاز كبريتيد الهيدروجين في نطاق كبير من الصناعات البترولية بالاضافه الى مخاطره الكبيره اصبح تطوير اجهزه مرنه وذكيه ورخيصه الثمن كحساسات لغاز كبريتيد الهيدروجين هدف لكثير من الدراسات من هذا المنطلق تم التركيز في هذا البحث على تطوير اجهزه استشعار كهروكيميائيه لقياس تركيز غاز كبريتيد الهيدروجين . تم تحضير بوليمر البوليبيرول ودمجه بجسيمات نانويه من كل من اكسيد النحاس CuO واكسيد القصدير SnO₂ بطريقه . Insitu-polymerization تم دراسة التركيب الكيميائي و المظهر السطحي و المورفولوجي باستخدام كل من جهاز حيود الأشعة السينيه XRD ، الميكروسكوب الألكتروني الماسح HRTEM ، التحليل الطيفي للأشعه تحت الحمراء FT-IR . تم حساب حجم الجسيمات النانويه المحضره باستخدام التشتيت الضوئي الديناميكي (DLS) تم اختبار الحساسات المحضره في وجود تركيزات مختلفه من غاز كبريتيد الهيدروجين ودراسه مدى استجابتها عن طريق تغيير المقاومه الكهريبيه مع الوقت في درجه حراره الغرفه باستخدام جهاز Keithley electrometer. اظهرت النتائج الاستجابه العاليه لمركب Ppy/ SnO₂ للتركيزات المختلفه من الغاز بخلاف Ppy/CuO , Ppy